Check for updates

Received: 8 October 2021 | Revised: 16 November 2021 | Accepted: 21 December 2021

DOI: 10.1002/pc.26474

RESEARCH ARTICLE

Polymer COMPOSITES WILEY

Effect of stacking sequence and metal volume fraction on the ballistic impact behaviors of ARALL fiber-metal laminates: An experimental study

Ertan Kosedag[1] | **Murat Aydin**[2] | **Recep Ekici**[3]

[1]Department of Mechanical Engineering, Van Yuzuncu Yil University, Van, Turkey

[2]Department of Aeronautical Engineering, Erciyes University, Kayseri, Turkey

[3]Department of Mechanical Engineering, Erciyes University, Kayseri, Turkey

Correspondence
Ertan Kosedag, Department of Mechanical Engineering, Van Yuzuncu Yil University, 65080 Tusba, Van, Turkey.
Email: ekosedag@yyu.edu.tr

Abstract

Thanks to their superior mechanical properties, polymer matrix composites have gained considerable importance. In order to improve the impact resistance of polymer matrix composite materials, a new hybrid material known as fiber metal laminate (FML) has been developed. The aim of this study was to reveal the effect of stacking sequence (SS), metal volume fraction (MVF), and number of layers on ballistic resistance in fiber metal laminates (FMLs). Four types of FMLs in different sequences and MVF (25% and 50%) were produced with hot press and vacuum. Ballistic tests were carried out with a single stage gas gun system. The absorbed energy was calculated from the energy difference that occurred by taking into account the FMLs entry and exit velocity of the projectile and the projectile mass. Damage types were examined after ballistic testing. It was determined that the stacking sequence and MVF significantly affect the impact resistance of FMLs. It was determined that the metal layer, which first encounters the projectile, compared to the polymer matrix composite, is more effective on the impact resistance of FMLs, and the impact resistance increased with the increase of MVF. In addition, the increase in the number of layers, if the top layers remain the same, adversely affected the impact resistance. It was observed that the first layer that encounters the projectile and the amount of MVF have a significant effect on the ballistic impact strength. As the amount of MVF increases, the ballistic impact resistance increases.

KEYWORDS

ARALL, ballistic impact, fiber metal laminate, metal volume fraction, stacking sequence

1 | INTRODUCTION

Thanks to their high fatigue resistance,[1–4] specific strength,[5,6] corrosion resistance,[7,8] and specific stiffness,[9,10] polymer matrix composite materials have gained considerable importance since the Second World War. Despite these superior properties, the impact resistance of polymer matrix composite materials is weaker than metal alloys.[5] In order to improve the impact resistance of polymer matrix composite materials, a new hybrid material known as fiber metal laminate (FML) has been developed. FMLs are a kind of sandwich structure, obtained by combining appropriate layers of polymer matrix composite, polymer, metal, and metal alloy layers in a certain order. The first FML was developed at the Delft Technology University in the early 1980s.[11]

 © 2021 Society of Plastics Engineers.

FMLs are classified according to the type of fiber reinforced composite and metal sheet material used. While the most commonly used metal layers are aluminum and its alloys, polymer matrix composite layers are aramid, glass, and carbon fiber reinforced composites. The first developed FML was ARALL (aramid reinforced aluminum laminate), followed by GLARE (glass reinforced aluminum laminate), and CARALL (Carbon reinforced aluminum laminate) in a short time.[11–13] FMLs are used in many fields, especially in the aviation (wing, fuselage, tail sections, etc.) and defense industry applications (low and high velocity impacts).

FMLs have many advantages over conventional fiber reinforced composites, such as superior corrosion resistance, higher damage tolerance, durability and sustainability of structure under fatigue loading, low density, and most importantly high impact resistance.[14,15] Due to the fact that FMLs are made of metal and fiber reinforced composites, they exhibit many different damage modes under impact. While buckling and plastic deformation are caused by the metal layer, matrix cracking, fiber breakage, and stripping, are caused by the composite materials. In addition, delamination can occur between layers.[16,17] Different failure modes and damage mechanisms allow the energy generated from an impact to be dissipated. Thus, FMLs become more resistant to impact than composite materials.[18,19] Some studies conducted to investigate low, high, and ballistic resistances of FML can be found in Sadighi et al.[20–26] In the literature, it is possible to come across studies proving that aramid reinforcement is an effective reinforcement element on low velocity impact and ballistic resistance in polymer matrix composites. To illustrate some of these, Nunes et al.[27] produced aramid-epoxy composites in different geometries with vacuum and investigated the ballistic resistance of these composites. They reported that the energy absorption capacity and damage mechanisms strongly affected by the thickness of the composite. Karahan et al.[28] presented the following results regarding the ballistic resistance of aramid reinforced composite laminates in their study: A linear relationship was observed between ballistic limit, energy absorption and composite thickness. Apart from these, it is possible to come across studies examining the effect of hybrid composites obtained from natural reinforcement elements together with aramid on the impact behavior and studies proving that low-velocity impact energy amount has a significant effect on the impact resistance of aramid reinforced composites.[29,30]

The most common FMLs in the literature are GLARE, CARALL, and ARALL. CARALL applications are very limited due to the fact that carbon fiber and aluminum layer interfaces are highly susceptible to galvanic corrosion and thermal incompatibility between layers. Although ARALL and GLARE have many application areas, GLARE finds more applications because it is cheaper. However, considering ARALL's high shear strength and superior properties of aramid fibers, it is clear that it needs further investigation in terms of impact resistance. Impact resistances of FMLs are affected by many parameters, such as geometry, constituent materials, stacking sequence, fiber orientation, layer thickness, and volume fraction of composites or metals.

In this study, the effect of stacking sequence, metal volume fraction, and number of layers on ballistic resistance of FML were investigated experientially. For this, four types of FMLs in different combinations were produced with hot press and vacuum. Ballistic tests were carried out at two different velocities. Based on depth of penetration (DOP) and absorbed energies, FML impact resistance was evaluated and post impact failure was visualized.

2 | EXPERIMENTAL PROCEDURES

Aramid fiber reinforced composite and Al6061 T6 alloy were used in the production of the ARALL FMLs. The thicknesses of the Al 6061 T6 alloy used were 1.5 and 3 mm. Aramid reinforced composites are obtained from prepreg structure. The prepregs were 300 g/m^2 cross ply aramid fabric and 40% epoxy resin-impregnated materials. The final thickness of each ply of aramid reinforced composite after curing was 0.5 mm. Surface cleaning was applied to metal layers before FML production. It was first kept in an ultrasonic cleaner with ethyl alcohol for 5 min, then cleaned with acetone, and finally kept in a 100°C oven for 30 min to remove moisture. FML production was carried out with the hot press technique. In order to metal surfaces to bonding well with polymer matrix composites, after surface cleaning, multidirectional roughening was performed on metals with 450 grid sandpaper. With this method, the prepreg and metal layers were lined up and cured together, so there was no need to use an extra adhesive to keep the metal and composite together. FML productions were carried out under a pressure of 1 bar in a vacuum environment. The curing temperature was applied simultaneously with the pressure. For curing, 120°C was reached in 24 min with 5°C/min heating speed, and then 1 h was waited at 120°C. Finally, it was left to cool slowly in the oven.

In this study, four different ARAL FMLs were produced according to Al metal volume fraction and stacking sequence. These are presented schematically in Figure 1. The notation used to describe the FMLs are FYAX and AXFY; where A: Al 6061 T6, X: Number of Al 6061 T6 sheets, F: Aramid layers, and Y: Number of Aramid layers.

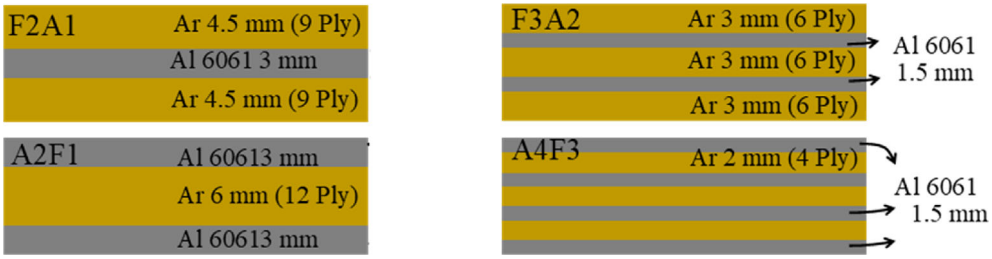

FIGURE 1 Schematic representation of different types of FML configurations

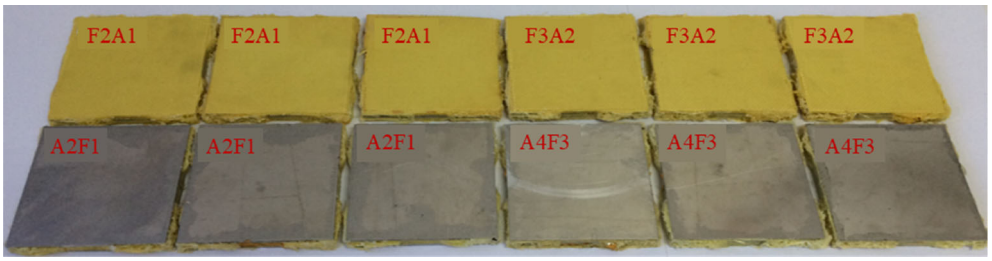

FIGURE 2 FML samples produced with hot press and vacuum

Accordingly, the first type sample (F2A1) consists of two aramid layers at the bottom and top, each 4.5 mm (9 ply) thickness, and 3 mm Al 6061 T6 layers in the middle. The total thickness of the F2A1 sample is 12 mm, and its 9 mm Aramid and 3 mm Al 6061 T6. The second type of sample (A2F1) consists of Al6061 T6 (3 mm) at the top and bottom and aramid reinforced composite (6 mm 12 ply) in the middle, in the reverse order of F2A1. The total thickness of the A2F1 sample is 12 mm.

The third type of sample (F3A2) consists of three layers of aramid-reinforced composite (3 mm 6 ply) and two layers of Al 6061 T6 (1.5 mm). Front and back surfaces are made of aramid reinforced composite. The total thickness of the aramid reinforced composite and Al 6061 T6 are 9 mm, 3 mm respectively, and the total thickness of the sample is 12 mm. Finally, the fourth type sample (A4F3) consists of 4 layers of metal (1.5 mm) and 3 layers of composite (2 mm, 4 ply) with Al 6061 T6 in the front and back. As the previous three samples, the total thickness of the A4F3 sample is 12 mm. The samples were produced in square geometry with dimensions of 100 × 100 mm^2. A total of 12 FMLs were produced in equal numbers from each type of sample (Figure 2).

Metal volume fractions (MVF) of F2A1 and F3A2 samples are 25%, while A2F1 and A4F3 samples are 50%. MVF is calculated as in Equation (1).[31]

$$\mathrm{MVF} = \frac{\sum t_{\mathrm{metal}}}{t_{\mathrm{FML}}} \quad (1)$$

The ballistic tests were performed with a single stage gas gun, shown in Figure 3A. The working principle of the setup is that helium gas compressed in certain amounts gives the projectile propulsion. Before the projectile enters the cabin where the target is fixed, it passes between two optical sensors and these optical sensors detect the entry velocity of the projectile. A Photran Brand high-speed camera was positioned at an angle to see the rear of the sample to detect the projectile exit velocity (Figure 3B). High-speed camera images made to determine the projectile exit velocity in ballistic tests were performed at 15000 frames per second. FSP (Fragment simulating projectile) projectiles that comply with MIL-DTL-46593[32] and NATO STANG 2920[33] standards were used. These projectiles were made of AISI 4340 steel and had 30 ± 2 Rockwell C hardness by heat treatment. Projectile shape and sabot parts used during firing are given in Figure 3C.

FMLs were fired at two different velocities, approximately 300 ± 10 and 500 ± 10 m/s. The exit velocities of the perforated samples were determined as a result of the analysis made with the high-speed camera. In the analysis, a known distance is defined as a reference and the exit velocity is determined by recording the position of the projectile at two different times. The difference between the projectile entry and exit velocities and the absorbed energy ($(\frac{1}{2} \times m \times V_{\mathrm{dif}}^2)$ m: bullet weight, V_{dif} difference in velocity) were calculated. Depth of penetration (DOP) of non-punctured FMLs was measured. Depth of penetrations were calculated by the program using the ImagJ open code software[34] by giving known lengths as reference and introducing the penetration regions. All FMLs were cut to take a cross-sectional view from the projectile hit.

3 | RESULTS AND DISCUSSION

The projectiles were fired at two different velocities, approximately 300 ± 10 and 500 ± 10 m/s, at each type

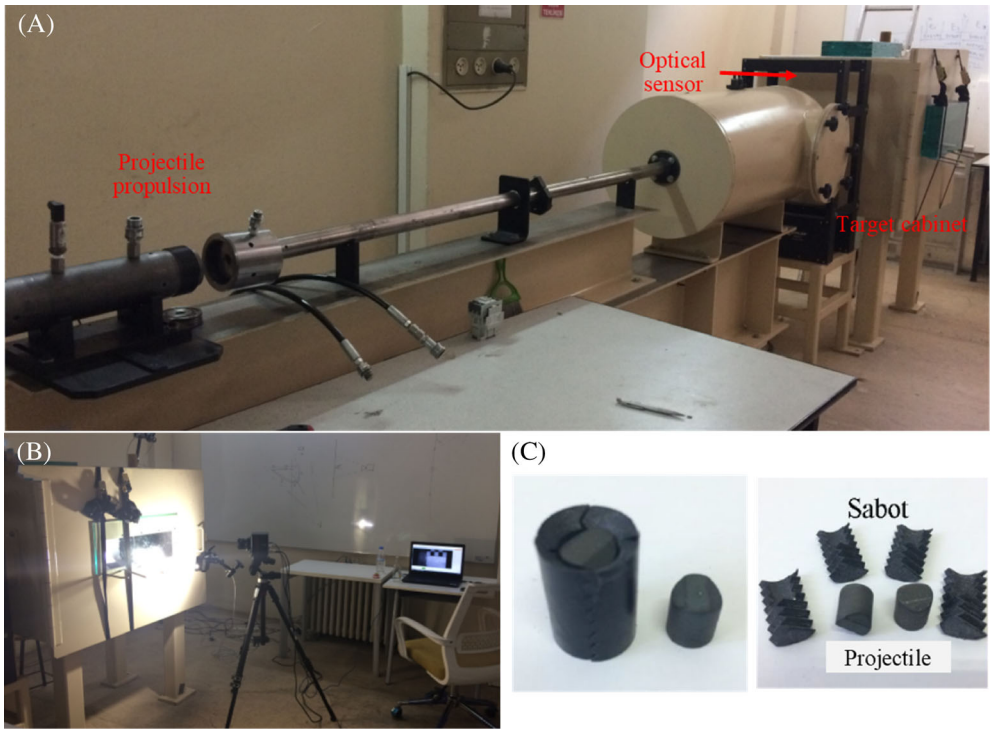

FIGURE 3 Ballistic test setup; (A) gas gun, (B) high speed camera, and (C) projectile-sabot system

FIGURE 4 Projectile exit velocity detection with high speed camera

of FML sample. Performed ballistic experiments will be explained through sample F2A1 (specimen located an Al 6061 T6 layer between two aramid-reinforced composite layers). The projectile exit velocity detection with a high-speed camera during the testing of the F2A1 FML sample at a projectile firing velocity of 500 ± 10 m/s is given in Figure 4. The projectile exit velocity in the perforated samples was measured by considering the position of the projectile coming out of the sample and the elapsed time as shown in Figure 4. Projectile exit velocity was measured from four different positions and its arithmetic mean was taken. As seen in Figure 4, exit velocities were measured as 314, 314, 296, and 310 m/s and the arithmetic mean was determined as $(314 + 314 + 296 + 310)/4 = 308$ m/s. Considering the projectile entry velocity 500 m/s, the difference between entry and exit velocities is 500–308 = 192 m/s. Therefore, it was concluded that the F2A1 sample slowed the projectile velocity by 192 m/s. In addition, the amount of energy absorbed can be calculated from Equation (2) by taking into account this velocity difference (V_{dif}) obtained, where the bullet weight is 0.0029 kg.

$$\frac{1}{2} \times m \times V_{\text{dif}}^2 \,(\text{J}) \tag{2}$$

Thus, it was determined that the F2A1 sample absorbs almost 53.5 J impact energy. Ballistic resistance of the non-puncture samples was determined by measuring depth of penetration. The weights of FMLs are different depending on the MVF. It is important to consider the weight of FMLs when comparing impact resistance. Therefore, it is more accurate to use the results of Equations (3) and (4) to compare the FML impact resistances.

$$\frac{\text{Absorbed energy}}{\text{FML}_w}\ (\text{J/g}) \tag{3}$$

$$\frac{\text{DOP}}{\text{FML}_w}(\text{mm/g}) \tag{4}$$

FML weights (FML_w), metal volume fraction, the projectile exit velocities of the perforated samples, and the DOP amounts of the non-perforated samples are given in Table 1. The absorbed energy calculated according to Equation (2) is presented in Table 2.

According to the ballistic results, it was determined that no specimen was punctured as a result of the shots at the first velocity (~300 m/s). All samples were perforated with the shots at the second velocity (~500 m/s). All of the samples tested at ~300 m/s and ~500 m/s were cut in two from where the projectile hit and the cross-sectional view was obtained (Figures 5, 6, 7, and 8). Front and back views of some samples are presented in Figure 9.

TABLE 1 DOP, PEV, MVF, and FML weight values

Depth of penetration (DOP), (~300 m/s)	Projectile exit velocity (PEV), (~500 m/s)	Metal volume fraction (MVF)	FML weight (FML_w)
(F2A1) 6.8 mm	(F2A1) 308 m/s	(F2A1) 25%	(F2A1) 175 g
(A2F1) 3.4 mm	(A2F1) 240 m/s	(A2F1) 50%	(A2F1) 210 g
(F3A2) 7.3 mm	(F3A2) 364 m/s	(F3A2) 25%	(F3A2) 175 g
(A4F3) 6.3 mm	(A4F3) 285 m/s	(A4F3) 50%	(A4F3) 210 g

TABLE 2 Some results obtained and calculated from the ballistic tests

Samples	Projectile exit velocity (PEV, m/s) for ~500 m/s	Velocity difference (V_{dif}, m/s), for ~500 m/s	Absorbed energy (J), for ~500 m/s	Absorbed energy/FML_w (J/g) for ~500 m/s	DOP/FML_w (mm/g) for ~300 m/s
F2A1	308	192	53.5	0.31	0.038
A2F1	240	260	98	0.47	0.016
F3A2	364	136	27	0.15	0.041
F4A3	285	215	67	0.32	0.030

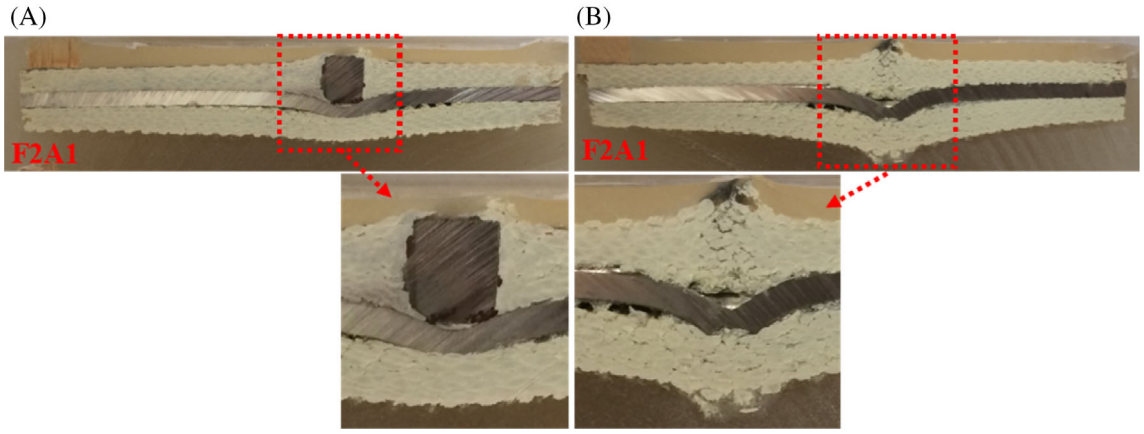

FIGURE 5 Cross-section views of the F2A1 sample as a result of the ballistic tests performed at firing a velocity of (A) ~300 m/s and (B) ~500 m/s

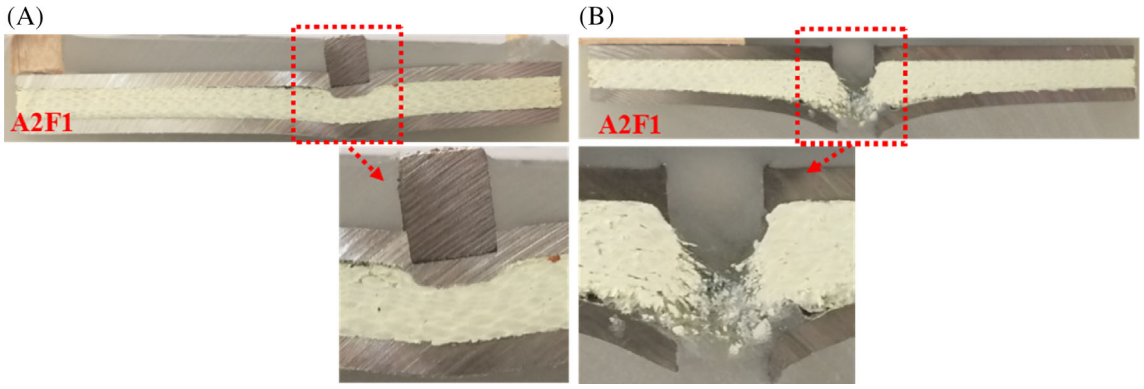

FIGURE 6 Cross-section view of the A2F1 sample as a result of the ballistic test performed at firing a velocity of (A) ~300 m/s and (B) ~500 m/s

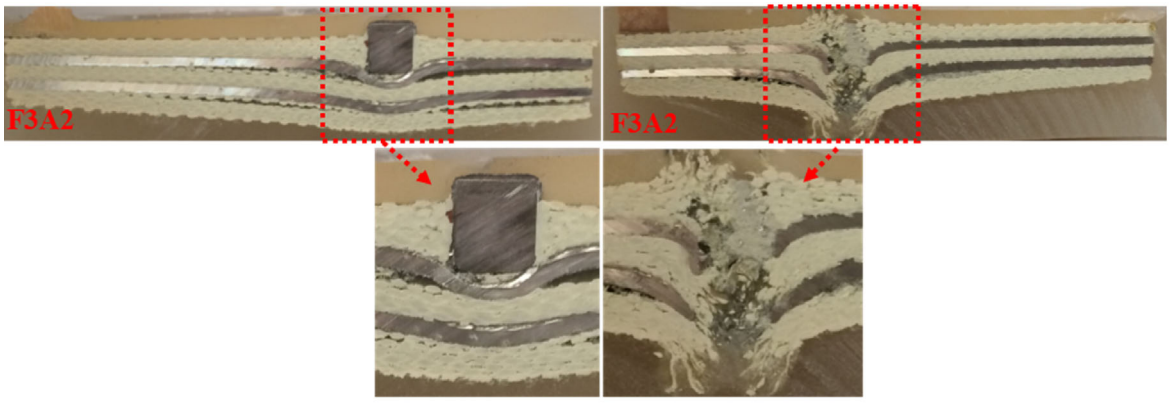

FIGURE 7 Cross-section view of the F3A2 sample as a result of the ballistic test performed at firing a velocity of (A) ~300 m/s and (B) ~500 m/s

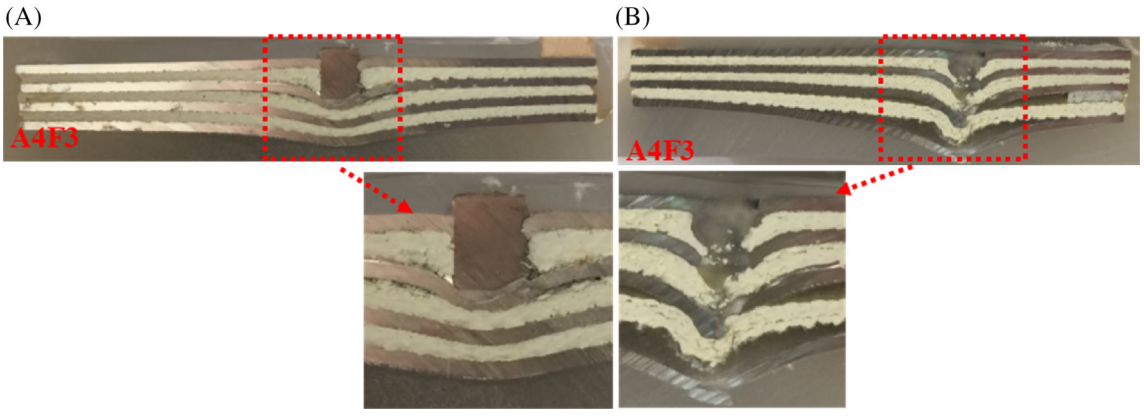

FIGURE 8 Cross-section view of the A4F3 sample as a result of the ballistic test performed at firing a velocity of (A) ~300 m/s and (B) ~500 m/s

In terms of impact resistance, the main parameter that distinguishes FMLs from conventional fiber reinforced composite materials and makes it superior is the added metal layers. Thus, in addition to the composite material damage, the damage to the metal layer and the delamination between these layers absorb and distribute the impact energy together. The types of damage commonly seen in FML structures are matrix cracking and fiber breakage/pullout/splitting caused by the composite material, while bulging, petalling, and plugging

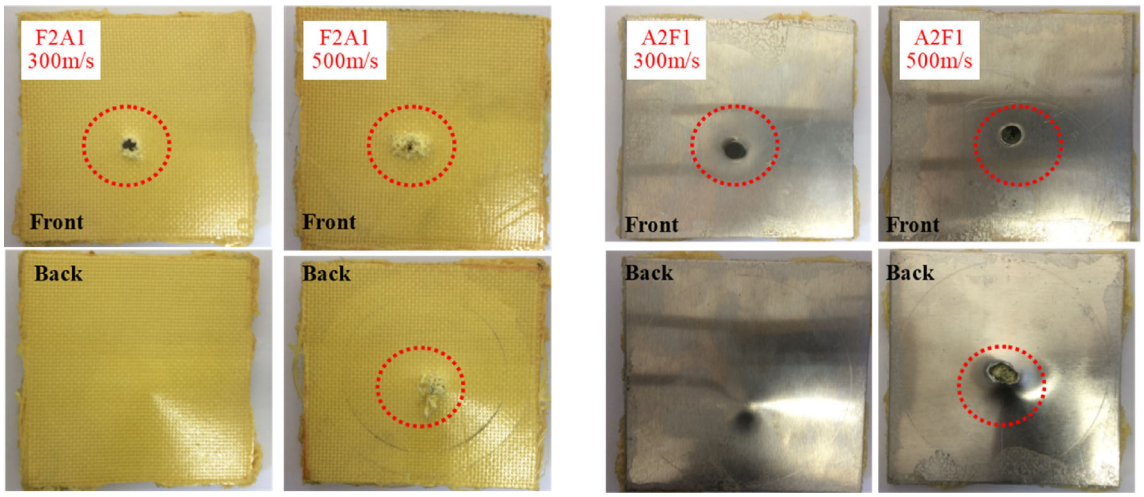

FIGURE 9 Front and back views of samples after ballistic testing

(generally by shearing load) are caused by the metal layer. In addition, delamination between metal and composite layers and thin plastic hinging can be seen around the impact area in the metal layer.

Figure 5A shows the cross-sectional images of sample F2A1 after the ballistic test. As seen in Figure 5A, sample F2A1 was not punctured as a result of the shot made at the velocity of ~300 m/s, whereas the sample was completely perforated at the shot velocity of ~500 m/s. The DOP that occurred in the F2A1 sample for firing velocity of ~300 m/s was measured as 6.8 mm. The projectile exit velocity from the F2A1 sample was determined as 308 m/s for firing velocity of ~500 m/s. In the F2A1 sample for firing velocity of ~300 m/s, the composite layer on the front was completely perforated. However, the metal layer in the middle layer underwent plastic deformation but no perforation was observed. Some swelling was detected in the back of the specimen. Furthermore, delamination between the metal layer and the composite layer was detected in a small amount. The brittle composite layer meeting the projectile reduced the velocity of the projectile and the ductile metal layer absorbed the remaining energy of the bullet by plastic deformation, so the projectile could be stopped. Figure 5B presents the cross-sectional images of sample F2A1 for firing velocity of ~500 m/s. It was observed that after the ballistic test, delamination between the composite sample and the metal layer, abundant fiber breakage and metal puncture, in addition to plastic deformation occurred.

The cross-sectional images of the second type sample are presented in Figure 6. Accordingly, as in the first type sample (F2A1), it was observed that sample A2F1 was perforated at the ~500 m/s velocity, whereas it was not perforated at the ~300 m/s velocity. However, when the DOP amounts and projectile exit velocity are compared, a significant difference stands out. DOP occurred in sample A2F1 was measured as 3.4 mm for firing velocity of ~300 m/s. The projectile exit velocity from the A2F1 sample was measured as 240 m/s for firing velocity of ~500 m/s. In the A2F1 sample for firing velocity of ~300 m/s, the metal layer, which is the top layer, failed due to the effect of shear forces. In addition, a low amount of plastic deformation was observed. In the A2F1 sample for firing velocity of ~500 m/s, the upper layer was perforated without excessive plastic deformation, the composite in the middle layer was completely damaged, and the lower layer metal was perforated by relatively more plastic deformation.

According to the results of F2A1 and A2F1 for firing velocity of ~300 m/s and ~ 500 m/s, sample A2F1 is more resistant in terms of impact resistance than the sample F2A1. The total thicknesses of these two types of samples are the same, but their MVFs are different. While the MVF of the F2A1 sample is 25%, that of the A2F1 sample is 50%. In addition, the layers that meet the projectile first are also different. Accordingly, the high MVF and the layer that first encounters the projectile is a ductile metal and make the sample superior in terms of impact resistance. It should be noted that with the increase of MVF, an increase in the weight of the sample occurs.

Figures 7 and 8 show cross-sectional views of samples F3A2 and A4F3, respectively. Unlike the first two types of FMLs (F2A1 and A2F1), the number of layers are increased in the F3A2 and A4F3 FMLs on the condition that the total thickness remains the same. When examined on a macro scale, all samples were perforated at the projectile firing velocity of ~500 m/s. However, when the DOP and projectile exit velocities were examined for further analysis, each sample exhibited different impact

resistance according to its variable parameters. For the projectile firing velocity of ~300 m/s, DOP amounts of the samples F3A2 and A4F3 are obtained as 7.3 mm and 6.3 mm, respectively. In addition, under projectile firing velocity of ~500 m/s, the projectile exit velocity of F3A2 and A4F3 samples was measured as 364 m/s and 285 m/s, respectively. For the projectile firing velocity of ~500 m/s, the upper layer of sample F3A2 was completely pierced and the second layer did not allow the projectile to pass by experiencing high plastic deformation. In A4F3, unlike F3A2, the second layer was pierced for the projectile firing velocity of ~300 m/s. The probable reason for this situation is that the composite layer is more brittle and therefore fails without sufficient plastic deformation.

In both the F3A2 and A4F3 FMLs for firing velocity of ~500 m/s, the metal layers on the front side underwent less plastic deformation than the ones on the back. The probable reason for this is that the velocity of the projectile gradually decreases and consequently, the shear forces decrease and the contact time increases. In addition, the increase in the amount of delamination with the increase in the number of layers is remarkable. When all the tests of F3A2 and A4F3 FMLs are compared, it can be said that the impact resistance of the A4F3 sample is better than the F3A2 sample, especially when it is examined according to both DOP amounts and projectile exit velocity. Front and back views of some FMLs are presented in Figure 9. Accordingly, the F2A1 projectile inlets and outlets were realized in a smaller area compared to A2F1, since the aluminum layer has a more ductile structure compared to the fiber reinforced polymer matrix composite.

From Table 1 and Table 2, it is seen that the FML with the highest impact resistance is A2F1 in terms of DOP (3.4 mm) and absorbed energy (98 J) values. If these

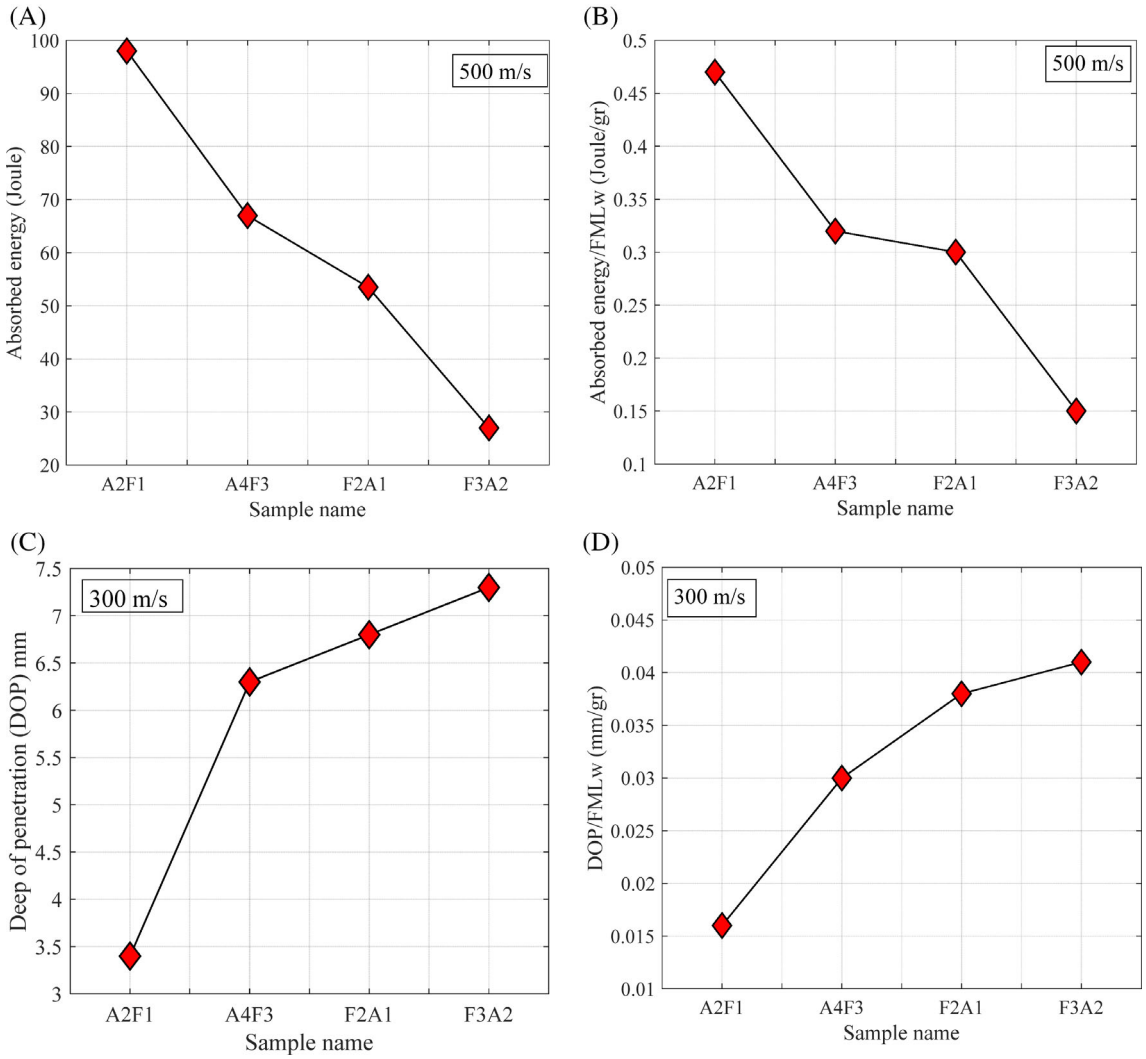

FIGURE 10 Ballistic test results: Comparison of FML impact resistances. (A) Absorbed energy, (B) absorbed energy/FML_w, (C) DOP, and (D) DOP/FML_w

values of A2F1 (3.4 mm, 98 J) are compared with F3A2 (7.3 mm, 27 J), which is the weakest FML, A2F1 is better by 114.7% and 263% in terms of DOP and absorbed energy than F3A2, respectively.

Variation of the impact resistance of FMLs is presented in Figure 10A,B,C,D in terms of the absorbed energy, absorbed energy/FML_w, DOP, and DOP/FML_w, respectively. Curves were drawn considering the sequential impact resistance of the FMLs. As shown in Figure 10A, FMLs were ranked according to the energy they absorb. Accordingly, FML A2F1 was the sample having the highest impact resistance for projectile firing velocity of ~500 m/s, whereas the lowest impact resistance was detected in the sample F3A2. The total thicknesses of all FMLs were kept equal. However, the MVF and weights of the FMLs are different. Considering that weight is a very important parameter in engineering applications, it was thought that it would be more accurate to compare FML impact resistances according to weight-free absorbed energy values. The energy absorbed/weight of the FMLs was processed and the results are presented in Figure 10B. In addition, the DOP amounts and weight-independent DOP/FML_w values of the samples that were not punctured, shot at first velocity, are given in Figure 10C and D, respectively. Considering the DOP amounts, the absorbed energy amounts, and their weight-independent values, it was determined that different types of FMLs showed similar impact resistance. Therefore, when the impact resistances of the FMLs are sorted from most resistant to weakest, it was obtained as A2F1, F4A3, F2A1, and F3A2. Similar results were found to be similar in all impact tests and repetitions.

As seen in Figure 10, the impact resistance of the A2F1 sample is superior compared to the others, the difference between F4A3 and F2A1 is relatively small, and F3A2 is quite weak compared to the others. When the FMLs are examined in terms of the layer that first encounters the projectile, it was found that the metal layer on top increases the impact resistance of the sample (A2F1 > F2A1, A4F3 > F3A2). In addition, it was determined that the increase of MVF has an important effect on the increase of impact resistance. Since increasing the amount of MVF will increase the weight, it will be correct to keep it at the optimum level. It is thought that, the reason for the increasing effect of the high MVF and the metal first layer on impact resistance is due to absorption of a large part of the projectile energy by plastic deformation and bending in the metal layer. The confusion of the projectile separated from the ductile metal layer with the brittle and stiffness composite layer causes an irregularity in the projectile move on. Thus, the impact energy originating from the projectile reflects back and causes delamination between layers. For this reason, some of the impact energy is absorbed by delamination. The combination of the ductility of the metal layer and the stiffness of the fiber reinforced composite material makes the FML structure superior in terms of impact resistance. If the top layer is the same, the increase in the number of layers in FMLs negatively affects the FML impact resistance (F2A1 > F3A2, A2F1 > A4F3). From this result, it is understood that the thickness of the different layers must be kept above a certain fraction in order to confuse the projectile motion and slow down its progress. It is also possible to see similar results in terms of damage mechanisms from the literature.[13,19] In addition, some studies[25,27,28] reported similar results on the effect of metal volume fraction, the number of layers, and the type of layer that first encountered the projectile on ballistic behavior. According to a study report by Park et al.[35] the projectile converts some of its energy into work and the remaining energy is absorbed by the target through elastic and plastic deformations. These results confirm our study in terms of energy absorption mechanism. The type of the first layer encountered by the bullet affects the ballistic resistance. In a study by Albuja et al.,[36] it has been stated that if the first layer meeting the bullet is a ductile metal, this configuration provides stability in terms of the sample's ballistic resistance. This is a result in agreement with our study.

4 | CONCLUSIONS

In this study, the effect of stacking sequence, metal volume fractions (MVF), and number of layers on the ballistic impact resistance of the fiber metal laminates (FMLs) were investigated. Four types of FMLs were produced with hot press and vacuum by using Al 6061 T6 as the metal layer and epoxy resin impregnated aramid prepregs as composite layer. Although the metal and composite layers were in different stacking sequences and thicknesses, all specimens were kept at the same overall thickness. Ballistic tests were performed at two different velocities. Impact resistances of FML specimens were determined by depth of penetration and absorbed energy, depending on the perforation status of the FML. In addition, considering that the FML weights are different, the amount of DOP and absorbed energy were also determined, independent of weight. Accordingly, in the study, A2F1 was determined as the FML with the highest impact strength, while F3A2 was determined as the FML with the lowest impact strength. It was observed that the first layer that encounters the projectile and the amount of MVF have a significant effect on the ballistic impact strength. As the amount of MVF increases, the ballistic impact resistance increases. In addition, the fact that the

layer that meets first with the projectile is metal, contributes to the ballistic impact resistance of FMLs. Furthermore, the increase in the number of layers provided that the top layers remain the same, adversely affected the impact resistance.

CONFLICT OF INTEREST

All authors declare that they have no known competing financial interests or personal relationships that could appear to have influenced the work reported in this paper.

DATA AVAILABILITY STATEMENT

The authors confirm that the data supporting the findings of this study are available within the article and its Supporting Information. Raw data that support the findings of this study are available from the corresponding author, upon reasonable request.

ORCID

Ertan Kosedag https://orcid.org/0000-0002-5580-0414
Recep Ekici https://orcid.org/0000-0002-4420-8431

REFERENCES

[1] A. P. Mouritz, M. K. Bannister, P. J. Falzon, K. H. Leong, *Compos. Part A: Appl. Sci. Manuf.* **1999**, *30*(12), 1445.
[2] Y. E. Ma, H. Hu, Experimental and numerical investigation of fibre-metal laminates during low-velocity impact loading. in *ICF13*. Beijing, China **2013**.
[3] A. P. Mouritz, B. N. Cox, *Compos. Part A: Appl. Sci. Manuf.* **2000**, *31*(1), 1.
[4] A. P. Mouritz, K. H. Leong, I. Herszberg, *Compos. Part A: Appl. Sci. Manuf.* **1997**, *28*(12), 979.
[5] P. D. Mangalgiri, *Bull. Mater. Sci.* **1999**, *22*(3), 657.
[6] R. F. Gibson, *Compos. Struct.* **2010**, *92*(12), 2793.
[7] J. Bienias, H. Debski, B. Surowska, T. Sadowski, *Comput. Mater. Sci.* **2012**, *64*, 168.
[8] P. Morgan, *Carbon Fibers and Their Composites (1st ed.)*, CRC Press, **2005**. https://doi.org/10.1201/9781420028744.
[9] M. F. S. F. de Moura, A. T. Marques, *Compos. Part A: Appl. Sci. Manuf.* **2002**, *33*(3), 361.
[10] S. Davey, R. Das, W. Cantwell, S. Kalyanasundaram, *Compos. Struct.* **2013**, *97*, 310.
[11] A. Vlot, J. W. Gunnink, *Fibre Metal Laminates: An Introduction*, Springer Science & Business Media, **2011**. https://doi.org/10.1007/978-94-010-0995-9.
[12] G. B. Chai, P. Manikandan, *Compos. Struct.* **2014**, *107*, 363.
[13] A. Afaghi-Khatibi, G. Lawcock, L. Ye, Y.-W. Mai, *Comput. Methods Appl. Mech. Eng.* **2000**, *185*, 173.
[14] T. Sinmazçelik, E. Avcu, M.€O. Bora, O. Ç Oban, *Mater. Des.* **2011**, *32* (7), 3671–3685.
[15] G. Wu, J.-M. Yang, *JOM* **2005**, *57*(1), 72.
[16] P. Compston, W. J. Cantwell, C. Jones, N. Jones, *J. Mater. Sci. Lett.* **2001**, *20*(7), 597.
[17] S. Heimbs, T. Bergmann, D. Schueler, N. Toso-Pentecote, *Compos. Struct.* **2014**, *111*, 158.
[18] A. A. da Costa, D. F. da Silva, D. N. Travessa, E. C. Botelho, *Mater. Des.* **2012**, *42*, 434.
[19] R. Das, A. Chanda, J. Brechou, A. Banerjee, *Woodhead Publ. Ser.* **2016**, *02*, 491.
[20] M. Sadighi, R. C. Alderliesten, R. Benedictus, *Int. J. Impact Eng.* **2012**, *49*, 77.
[21] P. Cortes, W. Cantwell, *J. Compos. Mater.* **2007**, *41*(5), 613.
[22] G. Caprino, G. Spataro, S. Del Luongo, *Compos. Part A: Appl. Sci. Manuf.* **2004**, *35*(5), 605.
[23] J. F. Laliberté, C. Poon, P. V. Straznicky, A. Fahr, *Int. J. Fatigue* **2002**, *24*, 249.
[24] S. Zhu, G. B. Chai, *Compos. Sci. Technol.* **2012**, *72*(15), 1793.
[25] A. S. Yaghoubi, Y. Liu, B. Liaw, *J. Thermoplast. Compos. Mater.* **2012**, *25*(2), 223.
[26] A. Seyed Yaghoubi, Y. Liu, B. Liaw, *J. Aerosp. Eng.* **2011**, *25*(3), 409.
[27] S. G. Nunes, R. Scazzosi, A. Manes, S. C. Amico, W. F. A. Junior, M. Giglio, *Int. J. Impact Eng.* **2019**, *132*, 103307.
[28] M. Karahan, A. Jabbar, N. Karahan, *J. Reinf. Plast. Compos.* **2015**, *34*(1), 37.
[29] Ö. Y. Bozkurt, A. Erkliğ, M. Bulut, *Polym. Compos.* **2018**, *39*(2), 467.
[30] E. Kösedağ, R. Ekici, *EJOSAT* **2021**, *28*, 84.
[31] A. S. Yaghoubi, B. Liaw, *Compos. Struct.* **2012**, *94*(8), 2585.
[32] MIL-DTL-46593 B (MR) w/AMENDMENT 1: **2008**. *Projectile, calibers .22, .30, .50, and 20mm fragment-simulating*.
[33] NATO STANAG 2920: **2003**. *Ballistic test method for personal armour materials and combat clothing*.
[34] ImageJ Graphics Software, *ImageJ*, **2018**. Available from https://imagej.nih.gov/ij/index.html.
[35] J. L. Park, B. I. Yoon, J. G. Paik, T. J. Kang, *Text. Res. J.* **2012**, *82*(6), 542.
[36] E. H. Albuja, J. A. Szpunar, A. G. Odeshi, *Compos. Part A: Appl. Sci. Manuf.* **2016**, *87*, 54.

SUPPORTING INFORMATION

Additional supporting information may be found in the online version of the article at the publisher's website.

How to cite this article: E. Kosedag, M. Aydin, R. Ekici, *Polym. Compos.* **2022**, *43*(3), 1536. https://doi.org/10.1002/pc.26474